COMMUNICATION

A photoresponsive graphene oxide–C_{60} conjugate†

M. Barrejón,[a] M. Vizuete,[a] M. J. Gómez-Escalonilla,[a] J. L. G. Fierro,[b] I. Berlanga,[c] F. Zamora,[c] G. Abellán,[d] P. Atienzar,[e] J.-F. Nierengarten,[f] H. García*[e] and F. Langa*[a]

An all-carbon donor–acceptor hybrid combining graphene oxide (GO) and C_{60} has been prepared. Laser flash photolysis measurements revealed the occurrence of photoinduced electron transfer from the GO electron donor to the C_{60} electron acceptor in the conjugate.

Owing to their remarkable electronic properties, the various allotropic forms of carbon have attracted an enormous attention in the field of materials science.[1] For example, photovoltaic devices made with all-carbon thin films incorporating fullerenes, carbon nanotubes (CNTs) and graphene oxide have shown promising efficiencies for light to electrical energy conversion.[2] In this particular case, the all-carbon nanocomposites were co-assembled in water to yield stable colloidal dispersions for thin film processing.[2] On the other hand, covalent hybrid nanostructures combining fullerenes and CNTs[3] were prepared and incorporated into photovoltaic[3] or optical limiting devices.[4] C_{60} has also been grafted onto graphene surfaces.[5] Interestingly, such conjugates have shown enhanced nonlinear optical performances when compared to their individual components.[5b] In another example, graphene oxide (GO) has been decorated with both C_{60} and Zn(II)-phthalocyanines (ZnPc).[6a] Photophysical studies have revealed the occurrence of photoinduced electron transfer (PET) from the ZnPc donor to the C_{60} acceptor suggesting that the GO scaffold is capable of mediating the electron transfer events

involving the two other partners.[6a] Recently, the electron-donating behaviour of few-layer graphene in covalent ensembles with electron-accepting phthalocyanines have also been shown.[6b] The possibility to use GO as an electroactive component,[7,8] namely as an electron donor, in a GO–C_{60} conjugate, remains an open question. To answer this question, we now report the synthesis and the photophysical properties of a covalent GO–C_{60} conjugate. Indeed, laser flash photolysis investigations revealed effectively the occurrence of PET from the modified GO sheets to the fullerene, thus demonstrating the possibility to develop covalent photoresponsive nanoconstructs exclusively based on carbon materials.

The preparation of the covalent graphene oxide–[60]fullerene conjugate (**GO–C_{60}**) is depicted in Fig. 1. The starting GO was purchased from Nanoinnova Technologies.[9] It was then modified with 4-(trimethylsilyl)ethynylaniline *via* an aryl diazonium salt reaction,[10] to yield **GO-TMS**. Subsequent cleavage of the TMS groups using tetra-*n*-butylammonium fluoride (TBAF) gave **GO-CCH**. Finally, fullerene building block $\mathbf{1}^{11}$ was grafted onto the modified GO scaffold using the Cu-catalysed alkyne-azide cycloaddition (CuAAC) reaction under the conditions optimized for the grafting of fullerene-containing azide onto carbon nanohorns[11] [$CuSO_4 \cdot 5H_2O$, sodium ascorbate in *N*-methyl-pyrrolidone (NMP)] (see ESI†). The resulting **GO–C_{60}** conjugate forms stable suspensions in solvents such as DMF, NMP and CH_2Cl_2 (Fig. S1, ESI†). The **GO–C_{60}** hybrid obtained was characterized by Fourier-transformed infrared (FT-IR) spectroscopy, Raman spectroscopy, high-resolution transmission electron microscopy (HR-TEM), atomic force microscopy (AFM) and X-ray photoelectron spectroscopy (XPS).

As shown in Fig. 2, Raman spectroscopy (λ_{exc} = 532 nm) of **GO** shows an intense tangential mode (G band) at 1585 cm^{-1} and a disorder-induced peak (D band) at 1356 cm^{-1}. These signals are observed at 1588 cm^{-1} and 1349 cm^{-1} in the spectrum of **GO-TMS**. As a consequence of the functionalization, the I_D/I_G ratio is slightly higher for **GO-TMS** (0.86) when compared to **GO** (0.73). The spectrum of **GO–C_{60}** shows the signatures of all its constituents: (i) 1594 cm^{-1} and 1355 cm^{-1} (GO sheet) and (ii) 1486 cm^{-1} (Ag(2) mode of C_{60}). It is worth noting that no further increase of the I_D/I_G ratio was observed when going from **GO-TMS** to **GO–C_{60}**, thus

[a] *Instituto de Nanociencia, Nanotecnología y Materiales Moleculares (INAMOL), Universidad de Castilla-La Mancha, 45071, Toledo, Spain. E-mail: Fernando.Langa@uclm.es*
[b] *Instituto de Catálisis y Petroleoquímica, Cantoblanco, 28049 Madrid, Spain*
[c] *Universidad Autónoma de Madrid, Departamento de Química Inorgánica, E-28049 Madrid, Spain*
[d] *Instituto de Ciencia Molecular (ICMol), Universidad de Valencia, 46980, Valencia, Spain*
[e] *Instituto Universitario de Tecnología Química CSIC-UPV, Universidad Politécnica de Valencia, 46022 Valencia, Spain. E-mail: hgarcia@qim.upv.es*
[f] *Laboratoire de Chimie des Matériaux Moléculaires, Université de Strasbourg et CNRS, (UMR 7509), Ecole Européenne de Chimie, Polymères et Matériaux, 25 rue Becquerel, 67087 Strasbourg Cedex 2, France*
† Electronic supplementary information (ESI) available: Experimental details, XPS and IR spectra, CV data, and transient absorption spectra. See DOI: 10.1039/c3cc49589b
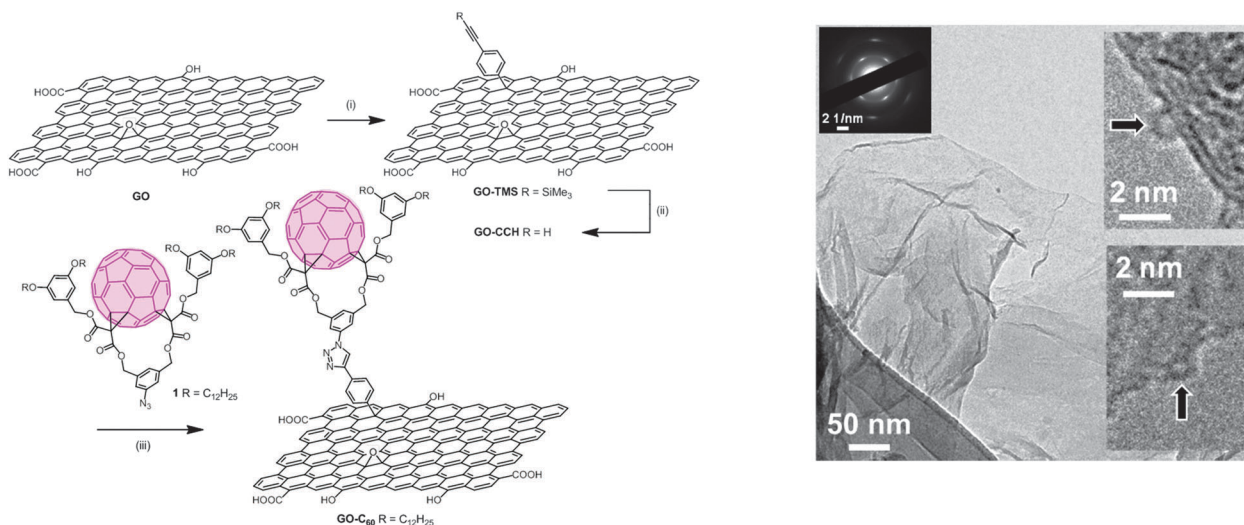
Fig. 1 (left) Preparation of **GO**–**C$_{60}$**. Reagents and conditions: (i) 4-(trimethysilyl)ethynylaniline, isoamyl nitrite, NMP, 70 °C, 24 h; (ii) TBAF, THF/NMP, rt, 1 h; (iii) CuSO$_4$·5H$_2$O, sodium ascorbate, NMP, 70 °C, 48 h. (right) HR-TEM images of **GO**−**C$_{60}$** and its corresponding SAED pattern. Insets on the right show spherical C$_{60}$ units highlighted with arrows.
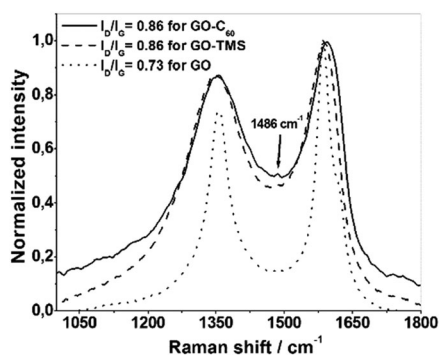
Fig. 2 Raman spectra (λ_{exc} = 532 nm) of **GO** (dotted line), **GO-TMS** (dashed line) and **GO**−**C$_{60}$** (solid line). The spectra are normalized to the peak intensity of the G band.

confirming that the cycloaddition reaction occurred onto the triple bonds of **GO-CCH** rather than directly onto the GO surface. The formation of **GO**–**C$_{60}$** was also evidenced by XPS (Fig. S2–S6, Tables S1 and S2, ESI†). In particular, the high-resolution N 1s spectrum of **GO**–**C$_{60}$** displays two components: (i) a major one at a binding energy of 399.9 eV, belonging to the two triazole N-atoms bound to C-atoms as nearest neighbors, and (ii) a minor one at 398.6 eV originating from the other remaining N-atom. In contrast, only one component is observed at 400.2 eV for azide **1**. These observations unambiguously prove that the azide residue of fullerene **1** is no longer present, thus, confirming the formation of triazole rings during the reaction leading to **GO**–**C$_{60}$**.[11] Based on the nitrogen content, measured by XPS, it was estimated that one fullerene is present per 161 GO atoms. FT-IR spectroscopy (Fig. S7, ESI†) further corroborated the results obtained by the previous techniques. Indeed, some of the diagnostic signals of precursor **1** were detected for **GO**–**C$_{60}$**. For example, the peaks around 2926 and 2855 cm^{-1} assigned to C–H stretching vibrations of alkyl chains. Importantly, the characteristic signal of azide groups (2092 cm^{-1})

could not be detected for **GO**–**C$_{60}$**, confirming again the successful functionalization of **GO-CCH** *via* the CuAAC reaction.[11]

HR-TEM shows that the morphology of **GO**–**C$_{60}$** was constituted by large GO sheets with lateral dimensions of several microns (Fig. 1 (right) and field emission scanning electron microscopy showing lateral dimensions over micron in Fig. S8, ESI†). Importantly, electron diffraction in selected areas reveals the characteristic GO hexagonal patterns. Moreover, the spherical structure of fullerene moieties grafted onto GO appears as circles with an inner diameter of *ca.* 0.7 nm in perfect agreement with the size of C$_{60}$ units (insets of Fig. 1 (right)).[11] Additional structural data were obtained by AFM investigations. Upon sonication of a suspension of **GO**–**C$_{60}$** in CH$_2$Cl$_2$ (60 min) and drop-casting deposition on SiO$_2$, AFM revealed a layered material with typical heights in the range of 7–10 nm (Fig. S10, ESI†). By increasing the sonication time, aggregation was further reduced leading to the observation of flakes with heights of *ca.* 4–6 nm (Fig. S9 and S11, ESI†).

The areas of the layers observed for **GO**–**C$_{60}$** are rather similar to those observed for the starting GO material, thus showing that the morphology of GO has been maintained during its functionalization (Fig. S13, ESI†).

The electrochemical properties of hybrid compound **GO**–**C$_{60}$** were investigated by cyclic voltammetry (CV). For the sake of comparison, electrochemical measurements were also carried out with C$_{60}$ and **1**. All the experiments were performed at room temperature in aceto-nitrile solutions containing tetra-*n*-butylammonium tetrafluoroborate (TBABF$_4$) as the supporting electrolyte. The first reduction is observed at −0.60 and −0.67 V for C$_{60}$ and **1**, respectively (Fig. S15, ESI†). Interestingly, this reduction is observed at −0.53 V for **GO**–**C$_{60}$** suggesting the existence of interactions between both moieties. A similar shift of the reduction potential has been already observed in a related carbon nanohorn–C$_{60}$ hybrid.[11] Under similar conditions the reduction potential of GO appears at −1.36 V.[12]

As typically observed for fullerene derivatives, compound **1** exhibits a weak emission at *ca.* 720 nm (Fig. 3A). This fluorescence
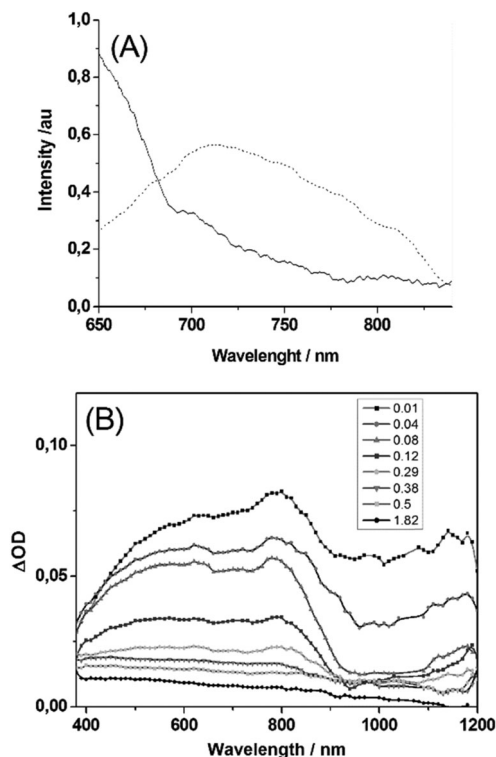
Fig. 3 (A) Fluorescence spectra of **1** (dashed line) and **GO**–C$_{60}$ (solid line) recorded in PhCN (λ_{exc} = 438 nm). (B) Transient absorption spectra of an N$_2$-purged benzonitrile solution of **GO**–C$_{60}$, depicted spectral traces are from 0.01 to 1.82 μs after the laser pulse (λ_{exc} = 355 nm).

signal is dramatically quenched in **GO**–C$_{60}$, suggesting the occurrence of excited-state interactions between the two forms of carbon in the conjugate. In order to elucidate the quenching mechanism, laser flash photolysis experiments were carried out on **GO**–C$_{60}$ in PhCN solutions (Fig. 3B). The results were compared to those obtained with compound **1** and **GO** (see ESI,† Fig. S17). Upon 355 nm nanosecond laser excitation of a PhCN solution of **GO**–C$_{60}$, the transient absorption spectra show a continuous absorption from 360 to 900 nm, peaking at 820 nm, as well as a continuous band from 1000 to 1200 nm. While the continuous absorption in the 400–800 nm region can be due to the combination of the spectra recorded for **GO** and **1**, the most salient feature is the intense NIR absorption recorded for **GO**–C$_{60}$.

The latter is ascribed to the absorption of fullerene radical anions. Similar transient absorptions have been recently observed in the NIR region upon PET in a modified GO derivative bearing C$_{60}$ and ZnPc subunits.[6] The temporal profile of the signals in the 360–900 nm zone was coincident, but the signal decay in the NIR region was slower indicating the presence of long-lived transient species, namely C$_{60}^{\bullet-}$.[13] GO is thus acting as an electron donor, however the oxidized GO has no characteristic absorption bands[14] in the visible region and the formation of GO$^{\bullet+}$ could not be monitored. It is also worth noting that no transient absorption was observed in the NIR region during control experiments using compound **1** in the absence of GO. Actually, the electron donor moiety generating C$_{60}^{\bullet-}$ must be GO and not the solvent.[14] Finally, the occurrence of photoinduced intramolecular electron

transfer in **GO**–C$_{60}$ deduced from the transient absorption experiments with **GO**–C$_{60}$ was further confirmed by bimolecular quenching experiments performed with mixtures of GO and C$_{60}$ (see ESI,† Fig. S20 and S21).

In conclusion, CuAAC chemistry allowed us to efficiently conjugate two nanoforms of carbon, and photoinduced electron transfer has been evidenced in the resulting **GO**–C$_{60}$ nanohybrid. Therefore, **GO**–C$_{60}$ nanoconstructs are appealing candidates for the preparation of all-carbon solar cells. Work in this direction is currently underway in our laboratories.

Notes and references

1 (a) *Fullerenes: principles and aplications*, ed. F. Langa and J.-F. Nierengarten, RSC, 2008; (b) *Carbon Nanotubes and Related Structures*, ed. D. M. Guldi and N. Martín, Wiley-VCH, Weinheim, 2010.
2 V. C. Tung, J.-H. Huang, I. Tevis, F. Kim, J. Kim, C.-W. Chu, S. I. Stupp and J. Huang, *J. Am. Chem. Soc.*, 2011, **133**, 4940.
3 For a review, see: M. Vizuete, M. Barrejón, M. J. Gómez-Escalonilla and F. Langa, *Nanoscale*, 2012, **4**, 4370.
4 N. Mackiewicz, T. Bark, B. Cao, J. A. Delaire, D. Riehl, W. L. Ling, S. Foillard and E. Doris, *Carbon*, 2011, **49**, 3998.
5 (a) X. Zhang, Y. Huang, Y. Wang, Y. Ma and Z. L. Yongsheng Chen, *Carbon*, 2008, **47**, 313; (b) Z. Liu, Y. Xu, X.-Y. Zhang, X.-L. Zhang, Y.-S. Chen and J.-G. Tian, *J. Phys. Chem. B*, 2009, **113**, 9681; (c) Y. Zhang, L. Ren, S. Wang, A. Marathe, J. Chaudhuri and G. Li, *J. Mater. Chem.*, 2011, **21**, 5386; (d) J. Pu, Y. Mo, S. Wan and L. Wang, *Chem. Commun.*, 2014, **50**, 469.
6 (a) S. K. Das, B. K. C. Chandra, K. Ohkubo, Y. Yamada, S. Fukuzumi and F. D'Souza, *Chem. Commun.*, 2013, **49**, 2013; (b) M.-E. Ragoussi, G. Katsukis, A. Roth, J. M. G. de la Torre, D. M. Guldi and T. Torres, *J. Am. Chem. Soc.*, 2014, **136**, 4593.
7 For examples of photoactive GO-donor systems in which the GO plays the role of an electron acceptor, see: (a) J. Malig, N. Jux, D. Kiessling, J.-J. Cid, P. Vázquez, T. Torres and D. M. Guldi, *Angew. Chem., Int. Ed.*, 2011, **50**, 3561; (b) L. Brinkhaus, G. Katsukis, J. Malig, R. D. Costa, M. García-Iglesias, P. Vázquez, T. Torres and D. M. Guldi, *Small*, 2013, **9**, 2348; (c) M.-E. Ragoussi, J. Malig, G. Katsukis, B. Butz, E. Spiecker, G. de la Torre, T. Torres and D. M. Guldi, *Angew. Chem., Int. Ed.*, 2012, **51**, 6421.
8 For an example of photoactive GO-acceptor system in which the GO plays the role of an electron donor, see: R. D. Costa, J. Malig, W. Brenner, G. Katsukis, N. Jux and D. M. Guldi, *Adv. Mater.*, 2013, **25**, 2600.
9 For more information see: www.nanoinnova.com.
10 S. Campidelli, B. Ballesteros, A. Filoramo, D. D. Diaz, G. de la Torre, T. Torres, G. M. A. Rahman, C. Ehli, D. Kiessling, F. Werner, V. Sgobba, D. M. Guldi, C. Cioffi, M. Prato and J.-P. Bourgoin, *J. Am. Chem. Soc.*, 2008, **130**, 11503.
11 M. Vizuete, M. J. Gómez-Escalonilla, J. L. G. Fierro, M. Yudasaka, S. Iijima, M. Vartanian, J. Iehl, J.-F. Nierengarten and F. Langa, *Chem. Commun.*, 2011, **47**, 12771.
12 E. L. K. Chng and M. Pumera, *Chem. – Asian J.*, 2011, **6**, 2899.
13 Detecting the building up of the fullerene anion was not possible as it is faster than the detection limit of the instrument.
14 (a) S. Kaniyankandy, S. N. Achary, S. Rawalekar and H. N. Ghosh, *J. Phys. Chem. C*, 2011, **115**, 19110; (b) J. Shang, L. Ma, J. Li, W. Ai, T. Yu and G. G. Gurzadyan, *Sci. Rep.*, 2012, **2**, 792.